0026-895X/95/010121-10$03.00/0

MOLECULAR PHARMACOLOGY, 47:121-130, 1995

Channel Inhibition by Alkanols Occurs at a Binding Site on the Nicotinic Acetylcholine Receptor

SUSAN C. WOOD, PETER H. TONNER,[1] ALBERTO J. DE ARMENDI, BIRGITTE BUGGE, and KEITH W. MILLER

Department of Anaesthesia, Massachusetts General Hospital (S.C.W., P.H.T., A.J.d.A., B.B., K.W.M.), and Department of Biological Chemistry and Molecular Pharmacology, Harvard Medical School (S.C.W., K.W.M), Boston, Massachusetts 02114

Received August 9, 1994; Accepted October 28, 1994

SUMMARY

The mechanism by which normal alkanols longer than ethanol inhibit cation flux through the transient open state of the nicotinic acetylcholine receptor (nAcChoR) is unknown. They might act nonspecifically either by perturbing the lipid bilayer or by binding to many low affinity sites. Alternatively, they might act in a mutually exclusive manner at a well defined site on the protein. To address this problem, a rapid assay of agonist-induced $^{86}Rb^+$ efflux from nAcChoR-rich *Torpedo* membrane vesicles was used that enabled the anesthetic-induced inhibition to be measured on a millisecond time scale, under conditions where the concentration of all ligands was raised in <1 msec, thereby avoiding complications due to desensitization. By measuring the inhibition constant of one agent as a function of the fixed concentration of a second agent, it is possible to distinguish between nonspecific action and mutually exclusive action. Our data are inconsistent with the hypothesis that 1-octanol and 1-heptanol act in a nonspecific manner, but they are consistent with the hypothesis that these two alkanols act in a mutually exclusive manner at a well defined site. The data suggest that the alkanols sterically compete for the site, but experimental limitations prevented a less plausible model, in which there is a strong negative allosteric interaction between separate octanol and heptanol sites, from being ruled out. Should the latter interaction occur, the data indicate that occupation of one alkanol site would decrease the affinity of the other by about 50-fold. The local anesthetic procaine is known to act in a mutually exclusive manner with the agonist self-inhibition site. We found that octanol and procaine acted at separate sites, which exhibited a negative heterotrophic interaction such that octanol reduced the affinity of procaine 6-fold. We conclude that octanol and heptanol inhibit cation flux through the channel of the nAcChoR by binding to a site (or a set of sites of equal affinity) whose location is distinct from, but allosterically coupled to, the agonist self-inhibition site.

Whether general anesthetics act by binding to an excitable protein by perturbing its surrounding bilayer or lipid/protein interface, or by some other mechanism has been the subject of much investigation. Although there is evidence for sites on soluble proteins of little neurological relevance, none has been obtained with excitable proteins because of difficulties such as the high degree of nonspecific binding, the transient nature of the active state, and the lack of overall structural information (reviewed in Refs. 1 and 2). Another difficulty with testing such a protein hypothesis is that the actual site of action in the central nervous system is unknown. However, a superfamily of ligand-gated ion channels, including the γ-aminobutyric acid receptor, nAcChoR, 5-hydroxytryptamine type 3 receptor, and *N*-methyl-D-aspartate receptor, are targets for general anesthetics. All of these receptors are thought to share structural features, and one of them, the nAcChoR, is available in sufficiently high purity to allow a test of the hypothesis.

A number of volatile general anesthetics and the *n*-alkanols longer than ethanol have been shown to inhibit cation flux through activated nAcChoR channels. In electrophysiological studies, inhibitory alkanols appear to decrease open channel lifetime (3), to reduce peak endplate currents, and to cause either increased or biphasic decay rates of miniature endplate currents (4, 5). In biochemical tracer ion flux studies, long-chain *n*-alkanols decrease agonist-mediated flux response, and their inhibitory potencies at the *Torpedo* receptor have been well documented (6).

Although it is apparent that these compounds act at a site or sites on the receptor/membrane complex distinct from the agonist site, there is no consensus on the nature of the inhibition site. Early studies postulated the involvement of lipid fluidity (4), but more recent studies tend to rule out a simple lipid-perturbation mechanism. For example, the dependence of inhibitory potency on the number of methylene groups in *n*-alkanols is steeper than that of membrane disordering (7),

This investigation was supported by a grant from the National Institute of General Medical Sciences (GM15904) to the Harvard Anesthesia Center, by the International Anesthesia Research Society (A.J.d.A.), and by the Department of Anesthesia, Massachusetts General Hospital.

[1] Present address: Abt. für Anästhesiologie, Universitäts-Krankenhaus Eppendorf, Martinistr. 52, W-2000 Hamburg 20, Germany.

ABBREVIATIONS: nAcChoR, nicotinic acetylcholine receptor(s); α-BTX, α-bungarotoxin; AcCho, acetylcholine; CCho, carbachol; QX-222, *N'*-(trimethylaminomethyl)-2',6'-xylidine; M2, transmembrane domain 2.

and inhibitory concentrations for the longer members of the series are below those that perturb bulk membrane lipids (6). Moreover, these actions vary qualitatively from alkanol to alkanol, suggesting a specificity of action typical of an alkanol/protein interaction (8). However, more subtle interactions at the lipid/protein interface are indicated by the observation that the concentration of halothane required to cause a given decrease in burst duration of the activated nAcChoR increases with the cholesterol to phospholipid ratio in the plasma membrane (9).

In contrast to the alkanols, there is good evidence that local anesthetics, which also noncompetitively inhibit the nAcChoR, act directly on the nAcChoR. Equilibrium binding studies (10) and ligand competition assays with a range of local anesthetics have identified high affinity sites that are allosterically coupled to the agonist site (11, 12). Photolabeling experiments add to this picture. A large body of electrophysiological data is consistent with the hypothesis that a site is also involved in the inhibition of the transient open state of the nAcChoR. At least for charged local anesthetics the site must lie in the transmembrane voltage gradient (4), a conclusion consistent with site-directed mutagenesis of the putative channel lining of the M2 region (13).

An alternative approach that allows the detection of even transitory anesthetic sites is based on characterizing the interactions between two inhibitors in a rapid kinetic $^{86}Rb^+$ efflux assay in *Torpedo* nAcChoR-rich vesicles, under conditions where the concentration of all ligands is raised in much less than 1 msec at the start of the assay (14, 15). This enables inhibitory concentration-response curves of one anesthetic to be measured in the presence of high concentrations of a second drug before the onset of complications such as fast desensitization. Using this technique, it was demonstrated that procaine interacts in a mutually exclusive manner with the inhibitory site of agonists (14). The hypothesis that alkanols act at such a site predicts that the inhibition constant for one alkanol would increase in the presence of a fixed concentration of a second alkanol, whereas for nonspecific action no such increase would be expected. Using this technique, we find that 1-octanol and 1-heptanol do act at a site that is separate from that occupied by procaine.

Materials and Methods

Preparation of *Torpedo* postsynaptic membranes. Postsynaptic membranes from freshly dissected electroplaques of *Torpedo nobiliana* (Biofish Associates, Georgetown, MA) were prepared using sucrose density gradient centrifugation at 4°, essentially as described by Braswell *et al.* (16). Membrane suspensions [5–10 mg of protein/ml, as determined by a modified Lowry method (17); 7–15 μM [^{3}H]AcCho binding sites, assayed as described (16)] were kept frozen at −80° for up to 6 months and were thawed within 48 hr of use.

Measurement of nAcChoR cation channel function. Cation channel function was assayed by measuring agonist-induced $^{86}Rb^+$ efflux from sealed native *Torpedo* electroplaque vesicles with a rapid quenched-flow technique, either as described by Forman *et al.* (18) or using a Biologique QMF-5 apparatus (Biologic, Claix, France); results were independent of the apparatus used. Because of the high surface density of receptors and the small internal volume of the vesicles, it was necessary to attenuate the agonist-induced flux response to prevent full equilibration of tracer within the assay time (7, 18); we refer to unattenuated vesicles as possessing excess response. This could be achieved in two ways. Either the number of active receptor/channel complexes was reduced by blocking with the effectively irreversible inhibitor α-BTX or, alternatively, measurements were made using untreated vesicle preparations in the presence of high levels of a noncompetitive blocking agent (see below for details). Receptor-mediated cation efflux was stimulated either with AcCho or with CCho, an AcCho analogue that is not hydrolyzed by acetylcholinesterase. In the former case vesicles were pretreated for 20 min with 0.1 mM diisopropylfluorophosphate to inhibit acetylcholinesterase, a treatment that did not influence the results. Total agonist-stimulated $^{86}Rb^+$ cpm [cpm(Ag,t)] were corrected for passive, time-dependent, $^{86}Rb^+$ leak from the sealed vesicles [cpm(leak,t)]. The corrected efflux response is expressed as F_A, the percentage of non-leak $^{86}Rb^+$ counts released.

$$F_A = \frac{\text{cpm(Ag},t) - \text{cpm(leak},t)}{\text{cpm(total)} - \text{cpm(leak},t)} \times 100\% \quad (1)$$

The alkanol-induced enhancement of $^{86}Rb^+$ leak from sealed vesicles was detected as an increase in filtrate cpm above the control leak level and was analyzed similarly to agonist-induced efflux (eq. 1).

Materials. α-BTX, buffer reagents, AcCho, CCho, and procaine hydrochloride were from Sigma Chemical Co. (St. Louis, MO), [^{3}H]-AcCho and ^{86}RbCl were from New England Nuclear (Boston, MA). 1-Heptanol and 1-octanol were obtained from Aldrich (Milwaukee, WI) and were at least 99% pure, as determined by gas chromatography. All alkanol solutions were prepared as described previously (6).

Analysis of alkanol concentration-inhibition curves. Alkanol concentration-inhibition curves were measured by using the rapid quenched-flow technique. Initial rate data were normalized to control values and fitted by nonlinear least-squares fitting to the logistic equation

$$k_{f(\text{nor})} = 1 - \frac{I^n}{i^n + K_i^n} \quad (2)$$

where I is the inhibitor concentration, K_i is the alkanol concentration causing 50% inhibition of maximum flux (or the apparent inhibition constant), and n is the Hill coefficient. Free alkanol concentrations were measured during each stage of an experiment by gas chromatography, as described previously (6). Statistical significance was judged by a two-tailed Student t test.

Analysis of agonist concentration-response curves. Agonist concentration-response curves were measured by using the rapid quenched-flow technique. Initial rate data were normalized to control values and fitted by nonlinear least-squares fitting to the logistic equation

$$k_{f(\text{nor})} = \frac{A^n}{A^n + \text{EC}_{50}{}^n} \quad (3)$$

where A is the agonist concentration and EC_{50} is the agonist concentration stimulating 50% of maximum flux. Statistical significance was judged by a two-tailed Student t test.

Additivity studies. The principles underlying this approach, which allows one to investigate the additive effects of two noncompetitive inhibitors at nAcChoR, have been outlined previously (14, 15). Briefly, the *Torpedo* efflux assay has a high degree of excess response, which conventionally is removed for quantitative studies by incubating vesicle preparations with stoichiometric amounts of the effectively irreversible antagonist α-BTX. This blocks a proportion of receptors, preventing their channels from being activated and reducing the rate of ion efflux to a level such that the measured integrated response is proportional to the fraction of activated channels (see Ref. 15). However, it is equally possible to remove this excess response from the experimental system by blocking activated channels with a noncompetitive inhibitor. If this noncompetitive inhibitor acts at the same site as the test inhibitor, then the apparent dissociation constant of the former drug is shifted to a higher concentration as the two drugs effectively compete for the same inhibitory site. Therefore, by reducing α-BTX blockade of nAcChoR-rich vesicles and instead removing excess flux response with a fixed concentration of an inhibitory alkanol, the additive effects of two alkanols can be determined.

As shown in Appendix 2, for sterically exclusive action (competition) of two inhibitors (B and C) the shift in the apparent dissociation constant of alkanol B is proportional to the concentration of C. Therefore, the clearest results are obtained at high concentrations of C. However, high concentrations of some anesthetics produce secondary effects on the experimental system, such as enhancing receptor desensitization and nonspecific tracer ion leak from membrane vesicles (15). Desensitization can be excluded by making flux measurements over such a short period of time that this process does not have time to develop. However, because it takes several seconds to collect and filter the quenched reacted membrane vesicles from the rapid mixing device, anesthetic-induced enhancement of background leak still remains a problem. For *n*-alkanols the chain-length dependence for channel inhibition is steeper than that for the membrane/buffer partition coefficient (6). On the other hand, alkanols longer than octanol are more difficult to work with because they adhere to the apparatus and significant quantities may partition into membranes. For this reason, longer alkanols were not studied. In practice, the mixtures of octanol and heptanol used did not enhance the leak by more than 10%. Shorter alkanols enhanced the leak more and were, therefore, excluded from this study.

Results

Effect of octanol on the initial rate of ion efflux from *Torpedo* vesicles. The initial rates of ion efflux in response to maximally activating concentrations of CCho (5 mM) were measured in the presence of a range of octanol concentrations. All experiments were performed with a single membrane preparation, and measured rates were normalized to control values obtained in the absence of any alkanol.

The treatment of initial rates is described in Appendix 1. Fig. 1 shows in detail the control initial rate measurement in the absence of added alkanol. Efflux rate is rapid and kinetics remain essentially linear for about 20 msec before an exponential decrease in the flux rate is observed. This flattening off of the flux profile is well documented (19, 20) and is thought to represent the onset of agonist-dependent fast desensitization (21).

The addition of octanol decreased the measured rate of ion flux from *Torpedo* vesicles. Data shown in Fig. 2 are plotted according to the linearized form of eq. A4 given in Appendix 1. The slope of the linear least-squares fit to this equation yields estimates of the initial rate of ion flux, k_f. Values of k_f are given in the legend to Fig. 2, normalized to the control [$k_{f(nor)}$]. Octanol concentrations in the range of 20–150 μM progressively reduced the rate of ion efflux; concentrations higher than this reduced flux to such an extent that the flux signal was inadequate for accurate measurements over the time scale of the experiment. Flux kinetics remained essentially linear for longer time periods at higher octanol concentrations (up to 50 msec with 150 μM octanol) (data not shown).

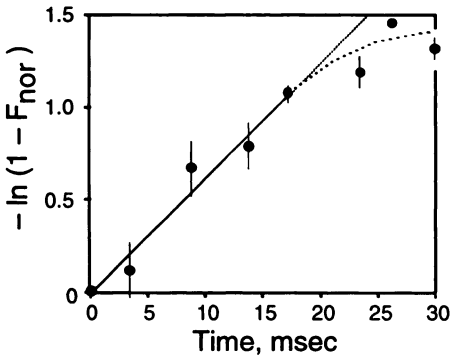

Fig. 1. Initial rate of ion efflux from *Torpedo* vesicles in response to 5 mM CCho. Vesicles were pretreated with α-BTX to block approximately 60% of AcCho sites. Flux responses (F_A) were measured using a quenched-flow assay, as described in the text. Data for channel activation up to 30 msec are shown normalized to the equilibrium flux response. Data up to 20 msec were fit by linear least-squares fitting ($r^2 > 0.90$) to yield an estimate of the initial rate of ion efflux (k_f) from this particular vesicle preparation, at 4°, of $k_f = 62.2 \pm 4.80$ sec^{-1}.

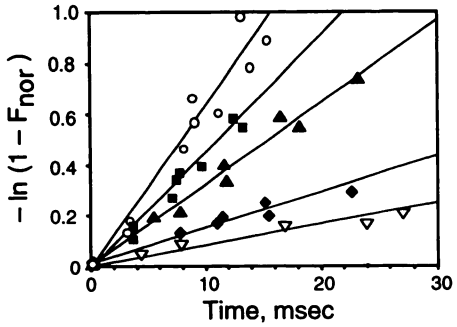

Fig. 2. Effect of octanol on the initial rate of ion efflux in response to maximal agonist stimulation. A single preparation of membranes vesicles (identical to that used in Fig. 1) was pretreated with α-BTX to block approximately 60% of AcCho sites. Measurements of flux responses were made at 4° in the presence of varying amounts of octanol using a rapid quenched-flow assay, as described in the text. Data for channel activation up to 30 msec are shown normalized to the equilibrium flux response and were fitted to an exponential equation (eq. A4) through an intercept of $y = 0$. The slopes of the plots, which are estimates of initial rates of ion efflux from *Torpedo* vesicles (k_f), are as follows: control (○), $k_{f(con)} = 62.2 \pm 4.80$ sec^{-1}, $k_{f(nor)} = 1$; 20 μM octanol (■), $k_{f(nor)} = 0.72 \pm 0.150$; 50 μM octanol (▲), $k_{f(nor)} = 0.51 \pm 0.118$; 100 μM octanol (◆), $k_{f(nor)} = 0.25 \pm 0.019$; 150 μM octanol (▽), $k_{f(nor)} = 0.13 \pm 0.017$.

Additive effects of heptanol and octanol on initial rates. The initial rates of ion efflux were measured as described previously, except that instead of blocking excess flux response by treating membranes with α-BTX a fixed concentration of heptanol was used. It was found that 0.2 mM heptanol produced about the same equilibrium flux response in a batch of untreated vesicles as measured for the toxin-blocked preparation used in the previous experiments. This concentration of heptanol was used to noncompetitively reduce flux response in the subsequent analysis of flux kinetics with octanol.

The form of the efflux kinetics in the presence of 0.2 mM heptanol did not appear to differ from those observed in α-BTX-blocked membrane preparations (compare Figs. 2 and 3), being linear from 2.5 to 15–20 msec, after which there was an exponential decrease of channel activity (data not shown). Because the channel kinetics do not appear to depend on whether excess receptor response is blocked by irreversible "competitive" inhibition (α-BTX) or by noncompetitive inhibition (heptanol), this is a good indication that the two sets of initial rate data for octanol can be directly compared.

Initial rates of ion efflux were measured in heptanol-blocked vesicles in the presence of various octanol concentrations. Data were normalized to control values and measurements of k_f were estimated as described above. Octanol concentrations in the range of 20–200 μM again progressively decreased the rate of ion efflux from heptanol-blocked vesicles, and some of these data are represented in Fig. 3.

The variation of $k_{f(nor)}$ with octanol concentration in both the presence and absence of heptanol was fitted by nonlinear least-squares analysis to a logistic equation (eq. 2), to estimate the

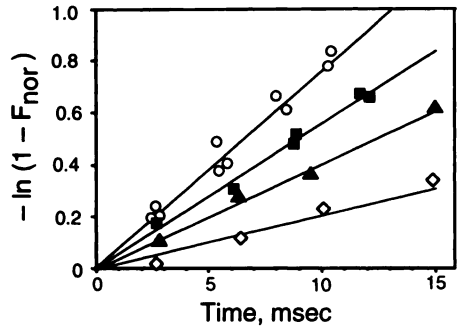

Fig. 3. Effect of octanol on the initial rate of ion efflux in response to maximal agonist stimulation in the presence of 0.2 mM heptanol. Measurements of flux responses were made at 4° in the presence of varying amounts of octanol using a rapid quenched-flow assay, as described in the text. All experiments were performed on untreated vesicles in the presence of 0.2 mM heptanol, to remove the excess response. Data for channel activation up to 15 msec are shown normalized to the equilibrium flux response and were fitted to eq. A4 (Appendix 1) through an intercept of $y = 0$. The slopes of the plots, which are estimates of initial rates of ion efflux from *Torpedo* vesicles (k_f), are as follows: control (○), $k_{f(con)}$ = 76.2 ± 5.03 sec^{-1}, $k_{f(nor)} = 1$; 20 μM octanol, $k_{f(nor)} = 0.84 \pm 0.090$; 50 μM octanol (■), $k_{f(nor)} = 0.74 \pm 0.068$; 66 μM octanol, $k_{f(nor)} = 0.61 \pm 0.045$; 100 μM octanol (▲), $k_{f(nor)} = 0.53 \pm 0.041$; 150 μM octanol, $k_{f(nor)} = 0.48 \pm 0.037$; 176 μM octanol, $k_{f(nor)} = 0.32 \pm 0.020$; 200 μM octanol (◇), $k_{f(nor)} = 0.27 \pm 0.034$.

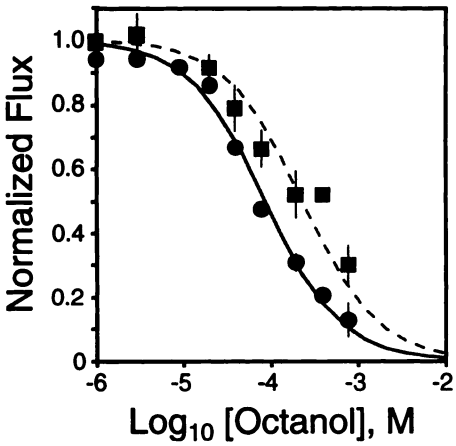

Fig. 4. Octanol concentration-response curves for efflux rates in the absence and presence of 250 μM heptanol. Efflux rates were estimated from determinations at a fixed time of 10 msec, using a single batch of membrane vesicles, in the presence of varying amounts of octanol. Two typical experiments are shown, in which vesicles were either pretreated with α-BTX (●) or blocked with 250 μM heptanol (■). Flux was normalized to the control value obtained in the absence of added octanol. *Curves* were fitted by nonlinear least-squares fitting to the logistic equation given in the text (eq. 2). Each *point* is from at least two determinations. *Vertical lines*, standard deviations, when larger then the symbols. The *curves* were drawn with Hill coefficients of 1, and their fitted parameters are as follows: control, $K_i = 87 \pm 4.6$ μM; +250 μM heptanol, $K_i = 246 \pm 24$ μM.

apparent dissociation constant for octanol inhibition of nAcChoR (data not shown). Octanol shows sigmoidal inhibition of the initial rate of ion efflux in response to maximal agonist activation, characterized by an apparent dissociation constant for the inhibitory site of octanol, K_i, of 44.8 ± 3.16 μM. This result is consistent with values previously obtained from quenched-flow integrated-flux measurements (6) and from electrophysiological experiments (5). In the presence of 200 μM heptanol, the inhibition curve for octanol was shifted to the right, resulting in an increase in the apparent dissociation constant of octanol for its inhibitory site to 107 ± 7.0 μM, a factor of 2.4 ± 0.23 greater than that observed in the absence of heptanol. The Hill coefficient for inactivation was not significantly altered in the presence of heptanol.

Dependence of inhibition constants of heptanol and octanol on the presence of the other alkanol. A fixed flux integration time between 10 and 15 msec was chosen in most subsequent experiments, to be in the linear range of flux responses (Fig. 2). In a few experiments two different integration times in this range were used. These more efficient assays allowed the examination of a wider range of alkanol concentrations in a given experiment, to more accurately determine the inhibition curves, which were then fitted to eq. A5 (Appendix 1) to obtain estimates of k_f.

Fig. 4 shows a typical experiment that confirms, using a wider range of octanol concentrations, the data from the kinetics experiments described above. In these experiments the flux integration time was 10 msec. In the control octanol experiment, where excess response was blocked with α-BTX, the apparent K_i was 87 ± 4.6 μM and in the presence of 250 μM heptanol the apparent K_i was 246 ± 24 μM, representing a significant shift of 2.8 ± 0.31-fold. Conversely, when heptanol inhibition curves were obtained in the presence or absence of 300 μM octanol (data not shown), the apparent K_i was shifted from 150 ± 12 to 590 ± 140 μM, again representing a significant shift, this time of 3.9 ± 0.98-fold.

To firmly establish the dependence of the apparent K_i values of the variable alkanol on the concentration of the fixed alkanol, it is desirable to examine as wide a concentration range of the latter as possible. As higher concentrations of alkanols were used two problems were encountered, both of which resulted from the wide range of concentrations needed to establish an inhibition curve with a Hill coefficient of about 1. First, the limited aqueous solubility of octanol and heptanol restricted the experimental concentration range and, second, the nonspecific leak increased. For example, above 800 μM octanol the leak correction increased above the controls and separate matched samples were necessary. In each such experiment the 100% inhibition point was confirmed in the absence of alkanols by using a high concentration of procaine (20 mM) as the final determination.

Fig. 5 shows the effect of various fixed concentrations of octanol on the apparent K_i (or IC_{50}) of heptanol. Eleven individual heptanol inhibition curves were determined over the concentration range of 0–300 μM octanol. The apparent K_i values obtained increased with increasing octanol concentration, in an essentially linear manner. The unconstrained linear least-squares fit passed through the control points and had a slope of 1.77 ± 0.18. Similarly, 12 individual octanol inhibition curves were determined at fixed concentrations of heptanol of 0–250 μM. The results are shown in Fig. 6. Once again, the apparent K_i values increased linearly with increasing fixed concentrations of the second alkanol (heptanol). The linear least-squares fit passed through the control points and had a slope of 0.74 ± 0.072. Taken together, these data show that the apparent K_i of each alkanol increases in the presence of the other alkanol. The slope of the solid regression lines are clearly different from the value of 0, which they would have if the actions of each alkanol were independent of the other. A more detailed consideration of these data and an explanation of the other lines is presented in the Discussion.

Interaction of octanol and local anesthetics at nAcChoR. In a previous study we showed that a local anes-

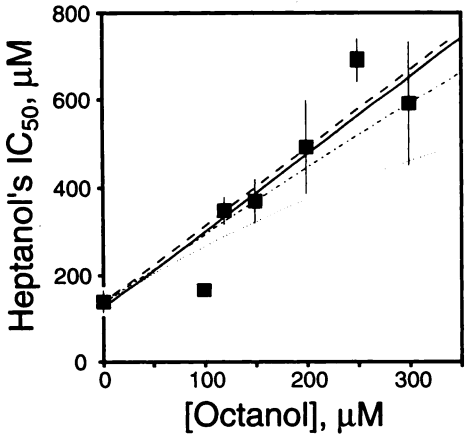

Fig. 5. Octanol and heptanol interaction at an inhibitory site on nAcChoR from *Torpedo*. The shift in the K_i of heptanol caused by the presence of fixed concentrations of octanol was determined (see Results). The control value is the mean ± standard deviation of six experiments, and the other *points* represent results from single experiments, with the errors from fitting to eq. 2 (the mean error for all curves was 13%). ——, Least-squares fit to the 12 individual experiments, with a slope of 1.8 ± 0.18 and an intercept of 120 ± 25 μM (r^2 = 0.91). – – –, Theoretical line calculated from eq. A9 (Appendix 2), assuming sterically exclusive action (competition) between heptanol and octanol. It has a slope of 1.7 ± 0.64 and an intercept of 130 ± 26 μM, where the errors are standard deviations calculated by error propagation from the apparent K_i values for each alkanol alone. · · · · · and – · – · –, Lines calculated for an allosteric model (eq. A10, Appendix 2) in which the affinity of heptanol for its site is reduced 10- and 50-fold, respectively, when the octanol site is occupied.

thetic, procaine, interacted in a mutually exclusive manner with the inhibitory site of the agonist suberyldicholine (14). To study the relationship between this site and the site of action of the alkanols, a series of 26 procaine inhibition curves were determined as a function of octanol concentration. Procaine had an apparent K_i of 280 ± 55 μM (mean and standard deviation of seven curves), close to that reported previously (14). Increasing concentrations of octanol between 50 μM and 1 mM were examined. Such high concentrations could be achieved because, unlike the alkanols, procaine had no effect on the nonspecific leak at concentrations used here. Fixed concentrations of octanol up to 700 μM could be examined satisfactorily, but above this concentration results were less reproducible. Nonetheless, at all concentrations above 100 μM, octanol significantly elevated the apparent K_i of procaine ($p \leq 0.01$). Linear regression gave a slope of 2.8 ± 0.38, as shown in Fig. 7. In a second series of experiments the inverse relationship was examined. The apparent K_i of octanol, which was found to be 70 ± 13 μM in five experiments, was significantly increased in the presence of 200 μM procaine, to 180 ± 36 in four experiments ($p \leq 0.001$).

In other studies we attempted to relate the alkanol site to that of other noncompetitive inhibitors whose sites have been identified by photolabeling or site-directed mutagenesis. Chlorpromazine, used in the photolabelng studies of Changeux *et al.* (22), had an apparent K_i of 0.1 mM, a concentration that enhanced the nonspecific leak dramatically. Therefore, additivity experiments with alkanols could not be performed. The quaternary local anesthetic QX-222, which was used in the reverse pharmacology studies of Lester and colleagues (13), was

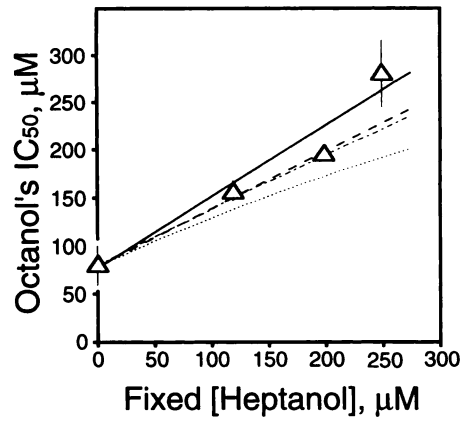

Fig. 6. Heptanol and octanol interaction at an inhibitory site on nAcChoR from *Torpedo*. The shift in the K_i of octanol caused by the presence of fixed concentrations of heptanol was determined (see Results). The control value and the 200 and 250 μM heptanol data are the mean ± standard deviation of six, two, and three experiments, respectively, and the other *point* represents results from a single experiment with the errors from fitting to eq. 2. ——, Least-squares fit to the 12 individual experiments, with a slope of 0.74 ± 0.072 and an intercept of 76 ± 11 μM (r^2 = 0.91). – – –, Theoretical line calculated from eq. A9 (Appendix 2), assuming sterically exclusive action (competition) between heptanol and octanol. It has a slope of 0.60 ± 0.20 and an intercept of 78 ± 21 μM, where the errors are standard deviations calculated by error propagation from the apparent K_i values for each alkanol alone. · · · · · and – · – · –, Lines calculated for an allosteric model in which the affinity of octanol for its site is reduced 10- and 50-fold, respectively, when the heptanol site is occupied.

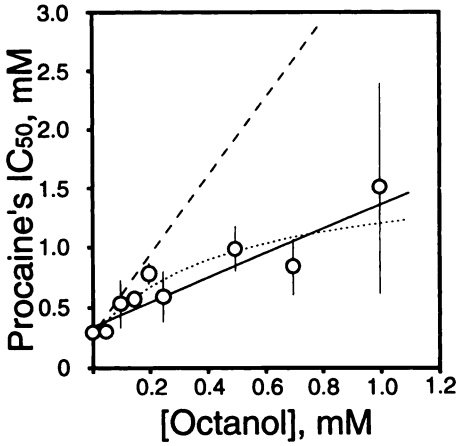

Fig. 7. Allosteric interaction of procaine and octanol on nAcChoR from *Torpedo*. The shift in the K_i of procaine caused by the presence of fixed concentrations of octanol was determined (see Results). The control value and those at 100, 250, 700, and 1000 μM are the mean ± standard deviation of seven, five, three, four, and three experiments, respectively, and the other *points* represent results from single experiments with the errors from fitting to eq. 2. ——, Least-squares fit to the 26 individual experiments, with a slope of 1.0 ± 0.18 and an intercept of 330 ± 83 μM (r^2 = 0.57). – – –, Theoretical line fitted to eq. A9 (Appendix 2), assuming sterically exclusive action (competition) between procaine and octanol. It has a slope of 3.3 ± 1.00 and an intercept of 280 ± 55 μM. · · · · ·, Line calculated by nonlinear least-squares fitting to the allosteric model (eq. A10, Appendix 2), in which the affinity of procaine for its site is reduced when the octanol site is occupied. The apparent K_i values for the procaine and octanol sites are taken from the experimental data (280 ± 55 and 86 ± 21 μM, respectively), and the apparent K_i for octanol when the procaine site is occupied (K_c' in eq. A10) is 510 ± 84 μM, a 6 ± 1.7-fold increase.

only a weak inhibitor, with a K_i of 2.7 ± 0.14 mM, rendering further studies of questionable utility. The absence of a transmembrane voltage in our vesicles is probably responsible for the low affinities encountered.

AcCho concentration-response curves in the presence of anesthetics. The concentration dependence of AcCho-induced $^{86}Rb^+$ efflux was studied from 0.3 μM to 8 mM, using a 10-msec efflux assay. The results are shown in Table 1. The control curve had a half-maximal flux concentration (EC_{50}) of 141 ± 33 μM and a Hill coefficient of 1.5 ± 0.26, a result consistent with previous work (18, 23). A concentration of octanol or procaine approximately equal to $1 \times K_i$, which reduced the maximum flux by half, did not significantly shift this curve along the concentration axis. A mixture of $1 \times K_i$ concentrations each of octanol and procaine did not further shift the curve relative to the values with $1 \times K_i$ concentrations of either agent, although relative to the control the increase in EC_{50} did approach significance ($p = 0.022$) and the Hill coefficient decreased ($p = 0.0054$).

Discussion

Evidence that octanol and heptanol do not act independently. Our major finding is that, when the inhibition by either octanol or heptanol is determined in the presence of a fixed concentration of the other, an increase in their apparent K_i values is observed (Figs. 5 and 6). This reciprocal relationship is observed at such short times that desensitization is excluded as an explanation.

For two inhibitors acting on a protein, several possible mechanisms of action may be distinguished. 1) Both may bind competitively to the same site and sterically displace each other. 2) Both may bind to separate, allosterically coupled binding sites, so that when one site is bound the other has lower affinity. 3) Both may bind to separate noninteracting binding sites. 4) Both may bind to one very large site, at which no interactions between bound ligands are observed (possible sites of action include the lipid bilayer or large hydrophobic patches on proteins, such as the lipid/protein interface or apolar clefts such as the gorge in acetylcholinesterase) (24).

Under the conditions of our experiments, the linear kinetic plots (Figs. 1–3) indicate that a steady state of open channels exists during the brief flux assay. The treatments of the models described above with the steady state approximation are given in Appendix 2 for reference. The results of such calculations are shown in Figs. 5–7.

Our data allow us to entirely rule out any model in which octanol and heptanol do not interact (mechanisms 3 and 4 described above), because these models predict that the presence of a second alkanol should not influence the apparent K_i of the first alkanol (see Appendix 2, model 3), a conclusion clearly at odds with the results shown in Figs. 5 and 6. This firm conclusion is consistent with indirect arguments advanced previously (6), based on the following observations. First, the Hill coefficients for inhibition by alkanols longer than hexanol are close to 1, suggesting that a single site or a set of sites of equal affinity mediate inhibition. This observation does not rule out the independent site mechanism (mechanism 3 described above), but our present data do so. Second, the dependence of the apparent K_i on alkanol chain length is steeper than that of lipid solubility or lipid disordering. Third, because the Hill coefficient is close to 1, a significant fraction of channels are inhibited at concentrations equivalent to one-tenth K_i and the degree of disordering of *Torpedo* membranes at such concentrations is very small (7). Taken together with our current work, these observations rule out any mechanism based on lipid-perturbation mechanisms or nonspecific adsorption to a large hydrophobic patch such as the lipid/protein interface (mechanism 4 described above).

Nature of the interaction between octanol and heptanol. Although the kinetic approach can conclusively rule out mechanistic models in which the alkanols act independently (mechanisms 3 and 4), it is less decisive at distinguishing between the remaining two mechanisms. These suggest either that heptanol and octanol act at a single inhibitory site on nAcChoR in a sterically exclusive manner or that a negative allosteric interaction occurs such that, upon binding of one alkanol to its site, the affinity of the second alkanol for its site at a different locus is dramatically reduced. In the following paragraphs we first consider how well our data support the sterically exclusive mechanism (mechanism 1 described above and Appendix 2, model 1) and then consider the allosteric model (mechanism 2 described above and Appendix 2, model 2).

The sterically exclusive model predicts that the measured inhibition constant of one alkanol should increase with the concentration of the second alkanol by an amount given by the ratio of the two individual, or unperturbed, apparent inhibition constants. The predicted linear relationship, which has no adjustable parameters, has been added to Figs. 5 and 6. It may be seen that the prediction is highly consistent with the data, within experimental error. In each series of experiments the slope obtained by least-squares regression is within 1 SD of the predicted slope (see legends to Figs. 5 and 6) and it may therefore be concluded that, unlike mechanisms 3 and 4, mechanism 1 is absolutely consistent with our experimental test.

At first sight the negative allosteric model (mechanism 2)

TABLE 1

Effect of noncompetitive inhibitors on the AcCho concentration-response curve for cation flux

Values are means ± standard deviations.

Inhibitor	AcCho concentration-response curve			p^a
	EC_{50}	Hill coefficient	Number of experiments	
	μM			
Control	141 ± 33	1.5 ± 0.26	5	
Octanol (100 μM)	177 ± 57	1.1 ± 0.20	4	0.27
Procaine (340μM)	215 ± 73	1.5 ± 0.29	3	0.09
Octanol (100 μM) + procaine (340 μM)	286 ± 109	1.0 ± 0.14	5	0.02

[a] Significance of shift in EC_{50}, compared with that of control.

can be ruled out because the observed relationship is linear, whereas eq. A10 (Appendix 2) predicts that the slope of the plot should decrease as the concentration of fixed alkanol increases. However, a more detailed examination of eq. A10 reveals that at low concentrations of the fixed anesthetic an approximately linear relationship is obtained. Because of technical limitations, in our experiments the fixed concentration of octanol did not exceed $4 \times K_i$, and simulations show that it is not possible to rule out a moderately strong negative allosteric interaction between an octanol site and a heptanol site. Our simulations show (Fig. 5) that, if the apparent dissociation constant of heptanol is progressively increased, it is not until a 10-fold change is used that there is a remote possibility of fitting the data. At that point the standard deviations of some points begin to overlap the prediction, but it requires a 50-fold decrease to obtain a good fit of the data. A ≥100-fold decrease gives predictions indistinguishable from the sterically exclusive model. These conclusions are also consistent with the data shown in Fig. 6. Thus, the negative allosteric model is not inconsistent with our data, and under these conditions we cannot differentiate between the case of true competition for a single inhibitory site and that of negative allosteric interactions between two separate sites. The technical difficulties associated with simultaneous use of both alkanols at high concentrations prevented us from using conditions that would have enabled a clearer distinction between the two models to be made.

Are such strong negative allosteric interactions likely at the nAcChoR? Interactions of this magnitude between the agonist site and the local anesthetic site are common, and the allosteric model cannot be rejected for this reason (25). However, this mechanism demands that each of the two sites be capable of distinguishing between octanol and heptanol, a possibility for which there is little precedent. Furthermore, the fact that the logarithm of the inhibitory concentrations of these alkanols is a strictly linear function of chain length (6) renders the hypothesis of separate sites inherently improbable.

In conclusion, this analysis indicates that our experimental data are most consistent with a model in which octanol and heptanol interact at a single inhibitory site in a sterically exclusive manner, but a mechanism in which alkanols at different sites exhibit a negative allosteric interaction, although unlikely, cannot be completely ruled out.

Interaction of octanol and procaine at nAcChoR from *Torpedo*. All agonists inhibit ion flux at much higher concentrations than are required to open the channel (23, 26). In a previous study using the same kinetic technique used herein, we showed that this inhibitory agonist site interacted with procaine in an apparently mutually exclusive manner (14). The question that we address in this section is whether the alkanol site is identical to that used by agonists and procaine. To answer this question we used procaine rather than agonists because full agonists like AcCho and CCho inhibit only at very high concentrations. In addition, relatively high procaine concentrations can be used without enhancing the leak of ions from the *Torpedo* vesicles. This allowed us to use much higher concentrations of one alkanol than we could when a second alkanol was to be added to the vesicles (see above). Indeed, we obtained procaine inhibition curves in the presence of fixed concentrations of octanol up to nearly $12 \times K_i$. Consequently, we were able to examine the octanol and procaine interaction more rigorously than in the case of octanol and heptanol.

Our data in Fig. 7 categorically rule out mechanisms 3 and 4; the data are inconsistent with either independent sites or a nonspecific mechanism. Furthermore, the sterically exclusive model (mechanism 1) (Fig. 7) accounts for the data only at the very lowest concentrations. The slope that this model predicts is 3 ± 1.2 times higher than the slope obtained by linear regression, and the model can therefore also be ruled out categorically. Because of the wide distribution of data, it was possible in this case to fit the allosteric model to eq. A10 (Appendix 2) by nonlinear least-squares fitting. A satisfactory fit was obtained and is shown in Fig. 7. The model predicts that the apparent K_i for octanol (K_C' in eq. A10) is increased about 6-fold when the procaine site is occupied.

Thus, we can conclude unequivocally that procaine and octanol inhibit AcCho-stimulated ion flux at separate sites, which exhibit a weak negative heterotrophic interaction. Equilibrium binding studies have previously demonstrated allosteric interactions between alkanols and the agonist and local anesthetic sites (10, 27, 28), but these likely reflect the nonspecific desensitizing action of the alkanols, rather than action at a specific alkanol site. Only one recent study has examined this question in the functional transient states of the nAcChoR (29). Those workers reported that the duration of open channel block by QX-222 was increased by either butanol or diethylether. Such a positive heterotrophic interaction is consistent with these general anesthetics not binding at the QX-222 site.

Possible locations of the alkanol inhibitory site. Our data show that the alkanol site must be distinct from the procaine site. Because we were unable to use charged noncompetitive local anesthetics, such as QX-222 and chlorpromazine (see Results), as a reference point, we cannot say whether the alkanol site is distinct from their site on the transient states of the nAcChoR, which is in a serine-rich region of the M2 helices (13, 22) thought to form the lining of the ion channel (30). The work of Dilger and Vidal (29) suggests that QX-222 and isoflurane do have separate allosterically coupled sites, but we do not know whether isoflurane uses the octanol site.

Procaine binds at the self-inhibitory agonist site (14), which preliminary data suggest is the quinacrine site (31). Time-resolved photolabeling indicates a site for quinacrine azide in the first transmembrane helix (M1) (32, 33), and equilibrium fluorescence experiments suggest that quinacrine binds to the lipid/protein interface (28, 34). It seems highly probable, therefore, that the alkanols do not bind at this site either.

A third possible alkanol site is a hydrophobic stretch of α-helix that is labeled by the hydrophobic photolabel 3-(trifluoromethyl)-3-*m*-([^{125}I]iodophenyl)diazirine in an agonist-sensitive manner (35). This region is bounded at the extracellular end of the M2 helix by the site labeled by meproadifen mustard (αGlu-262) and at the inner end, approximately 20 Å distant, by the serine-rich region (36).

It is possible that the whole intramembraneous portion of the nAcChoR is so cooperative that channel opening involves concerted movement in both the lipid/protein interface and the channel lumen. This would be consistent with the existence of a continuum of sites in which the binding of a single ligand is sufficient to influence the binding of any other ligand, a concept that has been explored previously (37). Nonetheless, the finding that heptanol and octanol act at a site distinct from both the procaine/agonist self-inhibition site and the QX-222 site should

prompt further site-directed mutagenesis and time-resolved photolabeling studies, which may resolve the issue.

Relevance of the *Torpedo* alkanol site to mechanisms of general anesthesia. One problem in espousing a protein hypothesis of general anesthetic action is that it has proved difficult to identify sites on functionally relevant proteins at physiologically relevant concentrations of anesthetic. Our most important finding is that such sites do exist and can be detected on transient conformational states of large integral membrane proteins. This means that protein theories of general anesthesia need no longer rely on studies of non-neuronal soluble proteins such as bovine serum albumin, β-lactoglobulin, and luciferase (reviewed in Refs. 1 and 2). The apparent K_i values of heptanol and octanol that we have measured are very close to their general anesthetic concentrations in tadpoles (230 and 60 μM, respectively) (38), suggesting that the site we have located, assuming that it exists on neuronal nAcChoR, may prove to contribute to the complex physiological state known as general anesthesia.

With the broad range of techniques available and the abundance of the nAcChoR from *Torpedo*, it should be possible to locate the alkanol site. Homology may then guide studies on other members of the superfamily. Whether such a broad attack will reveal elements of receptor structure common to each general anesthetic site, and therefore consistent with the classical unitary hypothesis, remains to be seen, but the complexity of general anesthetic pharmacology at the nAcChoR suggests that there may be no simple answer (6, 8).

Appendix 1. Estimations of Initial $^{86}Rb^+$ Efflux Rates

Measurements of $^{86}Rb^+$ efflux from α-BTX-blocked *Torpedo* vesicles were made after different periods of integration, starting from the shortest time obtainable with the rapid mixing apparatus (2–3 msec). Flux times were calculated from measurements of the flow rate through the rapid mixing device and the volume of the variable delay tube used (18).

From Ref. 20, the rate coefficient for ion flux before inactivation/desensitization, k_f, is given by

$$k_f = J \cdot R_o \cdot [A_2R]_o \tag{A1}$$

where J is the specific reaction rate for receptor-controlled ion translocation (characteristic of the receptor and independent of the type of activating ligand), R_o represents the moles of receptor sites per liter of internal vesicle volume (characteristic of the particular membrane preparation, and $[A_2R]_o$ is the fraction of active receptors in the open channel form.

At saturating agonist concentrations, all receptors are activated, $[A_2R]_o$ is constant, and the system is in steady state. In addition, for any particular membrane preparation J and R_o are constant. Thus, the movement of ions across the vesicle membrane is described by the following equation:

$$[Rb^+]_t = k_f \cdot t \tag{A2}$$

where $[Rb^+]_t$ is the number of ions translocated in time t.

However, because the vesicular internal volume is of limited size, the internal Rb^+ reservoir is limited and the rate of movement of ions out of the vesicle varies as the ion gradient across the membrane is depleted. Assuming a very large external volume, compared with the internal volume, i.e., such that $[Rb^+]_i - [Rb^+]_o \approx [Rb^+]_i$, then movement of $^{86}Rb^+$ across the membrane is approximated by pseudo-first-order kinetics.

$$-d\frac{[Rb^+]}{dt} = k_f \cdot [Rb^+]_i \tag{A3}$$

Correcting for nonreleasable $^{86}Rb^+$ counts and integrating flux response over time, in the absence of desensitization, the measured integrated flux F_{At} increases with time t,

$$F_{At} = F_{eq}[1 - \exp(-k_f \cdot t)] \tag{A4}$$

where F_{eq} is the measured flux response after long exposure to the maximum activating AcCho concentration.

The initial rate of ion efflux, k_f, can be estimated from the slope of a plot of $-\ln(1 - F_{At})$ versus t.

Estimated initial $^{86}Rb^+$ efflux rates from single-time point data were calculated as first-order approximations.

$$k_f = \frac{-\ln(1 - F_{At}/F_{eq})}{t} \tag{A5}$$

Because values of k_f are characteristic of a particular membrane preparation, all experimental values were normalized to paired control values and expressed as $k_{f(nor)}$, where

$$k_{f(nor)} = \frac{k_{f(alk)}}{k_{f(con)}} \tag{A6}$$

Appendix 2. Models of Interaction Between Anesthetic Sites

Model 1. Unimolecular, sterically exclusive action at a single site. With the high concentrations of agonist and short incubations used here, all receptors are bound and essentially all bound receptors are open, both because of the high opening probabilities of full agonists (39) and because of the lack of desensitization. Under these conditions, channel opening is fast, compared with measurement of the flux response (3), and the steady state approximation may be applied as in the scheme below, where inhibitors B and C act at the same site on the open form of the receptor R_o.

$$K_B = \frac{[B] \cdot [R]}{[BR_B]}$$

$$K_C = \frac{[C] \cdot [R]}{[CR_B]}$$

K_B and K_C are the apparent dissociation constants for B and C, respectively, and BR_B and CR_B are inhibited. The presence of inhibitor C increases the apparent dissociation constant of antagonist B

$$K_B^{app} = K_B\left(1 + \frac{[C]}{K_C}\right) \tag{A7}$$

This can be simplified either as

$$\frac{K_B^{app}}{K_B^{con}} = 1 + \frac{[C]}{K_C} \tag{A8}$$

a form that enables several sets of data to be displayed on a reduced plot, or as

$$K_B^{app} = K_B + \left(\frac{K_B}{K_C}\right)[C] \qquad (A9)$$

a form that predicts the relationship between the measured K_B^{app} and the concentration of the second alkanol.

Model 2. Allosteric interaction at separate binding sites. In the general model of antagonists B and C binding to receptor R at individual binding sites,

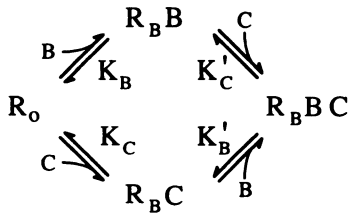

state R_o represents the open activated receptor, and R_BB, R_BC, and R_BBC are all inhibited. K_B and K_C represent the dissociation constants for B and C binding to the unoccupied receptor and K_B' and K_C' represent dissociation constants for B and C binding to the monoliganded receptor, respectively.

The apparent dissociation constant for B is given by

$$K_B^{app} = K_B \cdot \left[\frac{1 + ([C]/K_C)}{+ ([C]/K_C')}\right] \qquad (A10)$$

For negative allosteric interactions, occupancy of either antagonist site reduces the affinity of the other site, so that $K_C' \gg K_C$ and $K_B' \gg K_B$.

$K_B^{app} = K_B$ at [C] = 0, and the value of K_B^{app} increases at first linearly with low concentrations of C (because $[C]/K_C' \approx 0$). However, as [C] becomes larger, $[1 + ([C]/K_C)]/[1 + ([C]/K_C')]$ deviates from linearity and eventually asymptotically approaches a constant value of K_C'/K_C. Because the model demands that $K_B'/K_B = K_C'/K_C$, the asymptotic value is K_B'.

Thus, a plot of K_B^{app} versus [C] in the case of allosteric interaction would be hyperbolic. It is important to note that if $K_C' \gg K_C$ and the range of [C] used is only small, such that $[C]/K_C'$ is negligible, then the plot appears linear, because only the first part of the hyperbolic plot is measured.

Model 3. Action at noninteracting binding sites. This is a special case of the scheme described above, in which binding of each antagonist occurs independently of the other and therefore $K_B = K_B'$ and $K_C = K_C'$. Under these conditions, eq. A9 reduces to $K_B^{app} = K_B$ and no shift of K_B occurs with increasing [C].

References

1. Miller, K. W. The nature of the site of general anesthesia. *Int. Rev. Neurobiol.* **27**:1–61 (1985).
2. Franks, N. P., and W. R. Lieb. Molecular mechanisms of general anaesthesia. *Nature (Lond.)* **300**:487–493 (1982).
3. Dilger, J. P., and R. S. Brett. Actions of volatile anesthetics and alcohols on cholinergic receptor channels. *Ann. N. Y. Acad. Sci.* **625**:616–627 (1991).
4. Gage, P. W., and O. P. Hamill. Effects of anesthetics on ion channels in synapses. *Int. Rev. Physiol.* **25**:1–45 (1981).
5. McLarnon, J. G., P. Pennefather, and D. M. J. Quastel. Mechanism of nicotinic channel blockade by anesthetics, in *Molecular and Cellular Mechanisms of Anesthetics* (S. H. Roth and K. W. Miller, eds.). Plenum, New York, 155–164 (1986).
6. Wood, S. C., S. A. Forman, and K. W. Miller. Short chain and long chain alkanols have different sites of action on nicotinic acetylcholine receptor channels from *Torpedo*. *Mol. Pharmacol.* **39**:332–338 (1991).
7. Miller, K. W., L. L. Firestone, and S. A. Forman. General anesthetic and specific effects of ethanol on acetylcholine receptors. *Ann. N. Y. Acad. Sci.* **492**:71–87 (1987).
8. Liu, Y., J. P. Dilger, and A. M. Vidal. Effects of alcohols and volatile anesthetics on the activation of nicotinic acetylcholine receptor channels. *Mol. Pharmacol.* **45**:1235–1241 (1994).
9. Lechleiter, J., M. Wells, and R. Gruener. Halothane-induced changes in acetylcholine receptor channel kinetics are attenuated by cholesterol. *Biochim. Biophys. Acta* **856**:640–645 (1986).
10. Cohen, J. B., L. A. Correll, E. B. Dreyer, I. R. Kuisk, D. C. Medynski, and N. P. Strnad. Interactions of local anesthetics with *Torpedo* nicotinic acetylcholine receptors, in *Molecular and Cellular Mechanisms of Anesthetics* (S. H. Roth and K. W. Miller, eds.). Plenum, New York, 111–124 (1986).
11. Herz, J. M., D. A. Johnson, and P. Taylor. Interaction of noncompetitive inhibitors with the acetylcholine receptor: the site specificity and spectroscopic properties of ethidium binding. *J. Biol. Chem.* **262**:7238–7247 (1987).
12. Arias, H. R., C. F. Valenzuela, and D. A. Johnson. Quinacrine and ethidium bind to different loci on the *Torpedo* acetylcholine receptor. *Biochemistry* **32**:6237–6242 (1993).
13. Leonard, R. J., P. Charnet, C. Labarca, N. J. Vogelaar, L. Czyzyk, A. Gouin, N. Davidson, and H. A. Lester. Reverse pharmacology of the nicotinic acetylcholine receptor: mapping the local anesthetic binding site. *Ann. N. Y. Acad. Sci.* **625**:588–599 (1991).
14. Forman, S. A., and K. W. Miller. Procaine rapidly inactivates acetylcholine receptors from *Torpedo* and competes with agonist for inhibition sites. *Biochemistry* **28**:1678–1685 (1989).
15. Miller, K. W., S. C. Wood, S. A. Forman, B. Bugge, W. A. Hill, and V. Abadji. The nicotinic acetylcholine receptor in its membrane environment. *Ann. N. Y. Acad. Sci.* **625**:600–615 (1991).
16. Braswell, L. M., K. W. Miller, and J. F. Sauter. Pressure reversal of the action of octanol on postsynaptic membranes from *Torpedo*. *Br. J. Pharmacol.* **83**:305–311 (1984).
17. Hartree, E. R. Determination of protein: a modification of the Lowry method that gives a linear photometric response. *Anal. Biochem.* **48**:422–427 (1972).
18. Forman, S. A., L. L. Firestone, and K. W. Miller. Is agonist self-inhibition at the nicotinic acetylcholine receptor a nonspecific action? *Biochemistry* **26**:2807–2814 (1987).
19. Neubig, R. R., and J. B. Cohen. Permeability control by cholinergic receptors in *Torpedo* postsynaptic membranes: agonist dose-response relations measured at second and millisecond times. *Biochemistry* **19**:2770–2779 (1980).
20. Cash, D. J., H. Aoshima, E. B. Pasquale, and G. P. Hess. Acetylcholine-receptor-mediated ion fluxes in *Electrophorus electricus* and *Torpedo california* membrane vesicles. *Rev. Physiol. Biochem. Pharmacol.* **102**:73–117 (1985).
21. Forman, S. A., and K. W. Miller. High acetylcholine concentrations cause rapid inactivation before fast desensitization in nicotinic acetylcholine receptors from *Torpedo*. *Biophys. J.* **54**:149–158 (1988).
22. Changeux, J. P., J. L. Galzi, A. Devillers-Thiery, and D. Bertrand. The functional architecture of the acetylcholine nicotinic receptor explored by affinity labelling and site-directed mutagenesis. *Q. Rev. Biophys.* **25**:395–432 (1992).
23. Takeyasu, K., S. Shiono, J. B. Udgaonkar, N. Fujita, and G. P. Hess. Acetylcholine receptor: characterization of the voltage-dependent regulatory (inhibitory) site for acetylcholine in membrane vesicles from *Torpedo californica* electroplax. *Biochemistry* **25**:1770–1776 (1986).
24. Harel, M., I. Schalk, L. Ehret-Sabatier, F. Bouet, M. Goeldner, C. Hirth, P. H. Axelsen, I. Silman, and J. L. Sussman. Quaternary ligand binding to aromatic residues in the active-site gorge of acetylcholinesterase. *Proc. Natl. Acad. Sci. USA* **90**:9031–9035 (1993).
25. Taylor, P., P. Culver, R. D. Brown, J. Herz, and D. A. Johnson. An approach to anesthetic action from studies of acetylcholine receptor function, in *Molecular and Cellular Mechanisms of Anesthetics* (S. H. Roth and K. W. Miller, eds.). Plenum, New York, 99–110 (1986).
26. Sine, S. M., and J. H. Steinbach. Agonists block current through acetylcholine receptor channels. *Biophys. J.* **46**:277–284 (1984).
27. El Fakahany, E. F., A. T. Eldefrawi, and M. E. Eldefrawi. Nicotinic acetylcholine receptor desensitization studied by [^{3}H]perhydrohistrionicotoxin binding. *J. Pharmacol. Exp. Ther.* **221**:694–700 (1982).
28. Valenzuela, C. F., J. A. Kerr, and D. A. Johnson. Quinacrine binds to the lipid-protein interface of the *Torpedo* acetylcholine receptor: a fluorescence study. *J. Biol. Chem.* **267**:8238–8244 (1992).
29. Dilger, J. P., and A. M. Vidal. Cooperative interactions between general anesthetics and QX-222 within the pore of the acetylcholine receptor ion channel. *Mol. Pharmacol.* **45**:169–175 (1994).
30. Imoto, K., C. Busch, B. Sakmann, M. Mishina, T. Konno, J. Nakai, H. Bujo, Y. Mori, K. Fukuda, and S. Numa. Rings of negatively charged amino acids determine the acetylcholine receptor channel conductance. *Nature (Lond.)* **335**:645–648 (1988).
31. Arias, H. R., and D. A. Johnson. Localization of the agonist self-inhibitory binding site on the nicotinic acetylcholine receptor. *Biophys. J.* **66**:A10 (1994).
32. DiPaola, M., P. N. Kao, and A. Karlin. Mapping the α-subunit site photolabeled by the noncompetitive inhibitor [^{3}H]quinacrine azide in the active state of the nicotinic acetylcholine receptor. *J. Biol. Chem.* **265**:11017–11029 (1990).

33. Karlin, A. Structure of nicotinic acetylcholine receptors. *Curr. Opin. Neurobiol.* **3**:299–309 (1993).
34. Johnson, D. A., and J. M. Nuss. The histrionicotoxin-sensitive ethidum binding site is located outside of the transmembrane domain of the nicotinic acetylcholine receptor: a fluorescence study. *Biochemistry*, **33**:9070–9077 (1994).
35. White, B. H., and J. B. Cohen. Agonist-induced changes in the structure of the acetylcholine receptor M2 regions revealed by photoincorporation of an uncharged nicotinic noncompetitive antagonist. *J. Biol. Chem.* **267**:15770–15783 (1992).
36. Pedersen, S. E., E. B. Dreyer, and J. B. Cohen. Location of ligand-binding sites on the nicotinic acetylcholine receptor α-subunit. *J. Biol. Chem.* **261**:13735–13743 (1986).
37. Taylor, P., S. N. Abramson, D. A. Johnson, C. F. Valenzuela, and J. Herz. Distinctions in ligand binding sites on the nicotinic acetylcholine receptor. *Ann. N. Y. Acad. Sci.* **625**:568–587 (1991).
38. Firestone, L. L., J. C. Miller, and K. W. Miller. Tables of physical and pharmacological properties of anesthetics, in *Molecular and Cellular Mechanisms of Anesthetics* (S. H. Roth and K. W. Miller, eds.). Plenum, New York, 455–470 (1986).
39. Marshall, C. G., D. C. Ogden, and D. Colquhoun. Activation of ion channels in the frog endplate by several analogues of acetylcholine. *J. Physiol. (Lond.)* **433**:73–93 (1991).

Send reprint requests to: Keith W. Miller, Department of Anesthesia, Massachusetts General Hospital, Boston, MA 02114.